

# Photocatalytic Activity, Antibacterial Effect, and Self Cleaning Properties of TiO<sub>2</sub>/GO Thin Films

A. Jalaukan<sup>1,\*</sup>, S. M. Aldowaib<sup>2</sup>, A. S. Hamed<sup>3</sup>, B. Ghanbari Shohany<sup>4</sup>, R. Etefagh<sup>4</sup> and A. Khorsand Zak<sup>4,5</sup>

\* ali.jalaukhan@uokerbala.edu.iq

Received: May 2019

Revised: September 2019

Accepted: October 2019

<sup>1</sup> Department of Physics, College of Education for Pure Sciences, University of Kerbala Karbala, Iraq.

<sup>2</sup> Department of Sciences, Collage of Basic Education Al- Mustansiriyah University, Baghdad, Iraq.

<sup>3</sup> Department of Physics, College of Science, University of Kerbala, Karbala, Iraq.

<sup>4</sup> Borhan Nano Scale Company, Mashhad, Iran.

<sup>5</sup> Department of Physics, Nanotechnology Laboratory, Esfarayen University of Technology, Iran.

DOI: 10.22068/ijmse.16.4.53

**Abstract:** In this research, titanium dioxide/graphene oxide thin films at different concentration of graphene oxide (0.0, 0.015, 0.030, 0.045 and 4.5 g/mL) were prepared by spin coating method. Characterization of the samples was performed using X-ray diffraction and field emission scanning electron microscope and atomic force microscope. X-ray diffraction results showed that by adding the graphene oxide, the peak associated with (001) reflection was observed at the angle of 10.5°. The analysis of energy dispersive X-ray also confirmed the formation of graphene oxide sheets. Considering the excellent photocatalytic and antibacterial properties of titanium dioxide, the effect of adding different concentration of it on these properties has been investigated. The results showed that the presence of graphene oxide increases the inhibition of *Escherichia coli* bacterial growth.

**Keywords:** TiO<sub>2</sub>/GO, Spin Coating Method, Contact Angle, Antibacterial Properties, Photo Catalytic Properties.

## 1. INTRODUCTION

Titanium dioxide (TiO<sub>2</sub>) is very stable due to its physical and chemical properties [1-3]. It can be found in most of the cosmetic products [4]. It has many applications because of its unique properties, including electronic devices [5], gas sensors [6], solar cells [7-9], optical filters [10-11], and antibacterial and catalyst materials [12-17]. Recently, many researchers have focused on the development of photocatalyst thin film using TiO<sub>2</sub>, because it is inexpensive and non-toxic. Besides, it has high oxidative capacity, high stability, and therefore, many applications in environmental pollutions [18-19]. TiO<sub>2</sub> typically has three different crystalline structures called rutile, anatase, and brookite. Titanium atom is in contact with six oxygen atoms in all of these structures. The anatase and brookite structures are converted to rutile structure at temperature above 750°C; therefore, rutile structure is the most stable crystalline structure of TiO<sub>2</sub> [20-21].

Among the compounds that act as photo-catalyst, TiO<sub>2</sub> is the only suitable industrial material, because this material has an effective optical activity. It is also the most stable and low-cost photo-catalyst [22]. Due to the radiation of light by reducing the activation energy of the reaction, the photo-catalyst is used to accelerate the chemical reactions, while they remain unchanged. The photocatalytic activity is that their electrons are excited after absorption of the light and separated from their position. Thus, a hole remains that has a very high oxidizing property. At the same time, electrons have strong reduction properties. The electron-hole pair reacts with the molecules on the surface. A number of optical electrons and holes can reach the photo-catalyst surface and reduce or oxidize the adsorbed organic and non-organic species onto the catalyst surface.

TiO<sub>2</sub> is one of the materials that are widely used as self-cleaning surfaces. TiO<sub>2</sub> eliminates

surface contamination through two separate mechanisms: photo-catalysis and hydrophobic. During the photo-catalysis process, the chemical structure of organic pollutants and other impurities on the surface is broken down by absorbing sunlight. The hydrophilic property of the surface leads to create the water plates on the surface by reducing the contact angle that eliminates the contamination [23].  $\text{TiO}_2$  usually exhibits super-hydrophilic properties under ultraviolet light. Adding metals such as chromium, manganese, cobalt, and iron to  $\text{TiO}_2$  nanoparticles, the photo-catalytic degradation process of pigments in the visible light conditions can be done by using these nanoparticles.

A possible way to improve the properties of  $\text{TiO}_2$ , in order to use in practical applications, is the covering of the surface of  $\text{TiO}_2$  thin film with graphene oxide sheets. Graphene oxide is a 2D nano-material that is produced by oxidation of graphite. Graphene oxide is an oxide form of graphene sheets with oxygen functional groups such as hydroxyl, epoxy, carbonyl, carboxyl, and proxy. This material has been synthesized by the modified Hummers method. This method involves chemical or thermal peeling of graphite and ultrasonic in the presence of strong acids and oxidizing agents. The results of the researchers show that graphene oxide has very interesting and special properties. Their results also show that the addition of graphene oxide improves the antibacterial and self-cleaning properties of some structures [24].

Researchers have investigated the properties of titanium dioxide-graphene oxide thin films, in which the graphene oxide layer is first placed and then titanium dioxide is deposited on top of that layer. For example, in a study conducted by Baig et al., graphene oxide was first deposited. The titanium dioxide nanoparticles were then placed on it [27]. Based on our information, no similar research has been carried out in which the titanium dioxide thin-film is first deposited. The graphene oxide layer is then synthesized on titanium dioxide at different concentrations. Therefore, in the present work, we have investigated the effect of graphene oxide layer addition on the structural, morphological, photocatalytic, self-cleaning, and antibacterial properties of  $\text{TiO}_2$  thin films.

## 2. EXPERIMENTAL PROCEDURE

### 2.1 Preparation of $\text{TiO}_2$ Thin Film

At first, 75 mL of ethanol and 7.5 mL of acetic acid were mixed and stirred for 15 min by a magnetic stirrer. Then, 7.5 mL of titanium isopropoxide was added drop by drop to the above solution and stirred for another 15 min. In order to complete the chemical reactions, the resulting solution was kept and covered with foil for 24 hours at ambient temperature. On the other hand, the glass substrates were washed with 20% ethanol solution using ultrasonic for 30 min at 60 °C and then with acetone for 5 min. The prepared solution was coated by the spin coating method at 5000 rpm spinning speed for 1 min. This coating process was repeated 30 times. Finally, the obtained layers were calcined at 550°C for 1 hour.

### 2.2 Preparation of $\text{TiO}_2/\text{GO}$ Thin Films

At first, graphene oxide sheets were prepared from graphite using the modified Hummers method [28]. Then, the amount of 0.15 g, 0.30 g, 0.45 g, and 45 g of graphene oxide were dispersed in 10 mL of ethanol in ultrasonic bath for 10 min. After that, the graphene oxide solutions were coated on  $\text{TiO}_2$  layers by spin coating method at 5000 rpm for 1 min. The prepared films were dried at a temperature of about 40 °C-50 °C for 30 min. Finally, characterization was performed on the obtained samples.

### 2.3 Characterization

The crystal structures of the prepared thin films were characterized using XRD method by a D8 Advance Bruker YT diffractometer via  $\text{CuK}\alpha$  radiation in the range of 10° - 80°. The morphology of the layers was investigated using FESEM performed on MIRA3TESCAN-XMU microscope. X-ray microanalysis system was supported by a NanoTrace LN-Cooled Si (Li) detector for energy-dispersive X-ray spectroscopy (EDS) analysis. The surface morphology of the thin films was studied using AFM by Full Plus model from Ara-research company. Raman spectra were measured via Takram P50C0R10 using the 532 nm line of Nd:YAG laser as the excitation source.

### 3. RESULTS AND DISCUSSION

#### 3.1 Structural and Morphological Analysis

The X-ray diffraction patterns of the  $\text{TiO}_2/\text{GO}$  thin films at different concentrations of GO (0, 0.015, 0.030, 0.045 and 4.5 g/mL) are shown in Figures 1 (a-e), respectively. The diffraction peaks detected at  $2\theta = 24.68^\circ, 37.44^\circ, 47.56^\circ, 54.56^\circ, 55.6^\circ, 62.5^\circ, 68.6^\circ, 69.8^\circ, 74.75^\circ$  are related to (101), (004), (200), (105), (211), (204), (116), (220) and (215) planes, indicating the formation of  $\text{TiO}_2$  structure with anatase phase. By adding graphene oxide layer at concentrations of 0.015, 0.030, 0.045 g/mL (Figures 1b-d), no change was observed at the diffraction spectrum due to the very low concentration of graphene oxide. Therefore, the concentration of graphene oxide was chosen to be equal to 4.5 g/mL. Figure 1e shows the diffraction spectrum of  $\text{TiO}_2/\text{GO}-4.5\text{g/mL}$ . As can be seen, the graphene oxide peak at the angle of  $10.5^\circ$  related

to the (001) diffraction has been revealed, which confirms the presence of graphene oxide sheets on the  $\text{TiO}_2$  films. The X-ray diffraction pattern of graphene oxide nanosheets is also presented in figure 1f for comparison. All the diffraction peaks are sharp and well-defined, proposing that the prepared samples are well-crystallized.

Crystal sizes of the (001) diffraction peak were calculated by the Scherrer equation:

$$D_{hkl} = k\lambda/\beta\cos\theta$$

where  $D_{hkl}$  is the crystallite size,  $k$  is Scherrer's constant corresponding to the quality factor of the device measured with a reference for single crystal (0.9 for spherical particles),  $\lambda$  is the wavelength of X-ray,  $\beta$  is full-width at half-maximum (FWHM), and  $\theta$  is the Bragg angle [29]. The evaluated data are reported in Table 1.

Surface observations of the synthesized samples were done using FESEM, EDS, and AFM. In Figure 2, FESEM of  $\text{TiO}_2/\text{GO}$  thin films at different concentrations of 0, 0.015, 0.030, 0.04.5 and 4.5 g/mL are shown in figures 2 (a-e). The cross-section of the  $\text{TiO}_2$  thin film is shown in Figure 2f.

As shown in figures 2 (a-f), it is clear that the surfaces of the samples are very uniform, and the grains are homogeneously distributed with the similar sizes on the surface. After that, the graphene oxide layers are clearly observed in figures 2 (b-e). As expected, by increasing the concentrations of graphene oxide, the thickness of graphene oxide layers increases, and it covers the grains of titanium oxide.

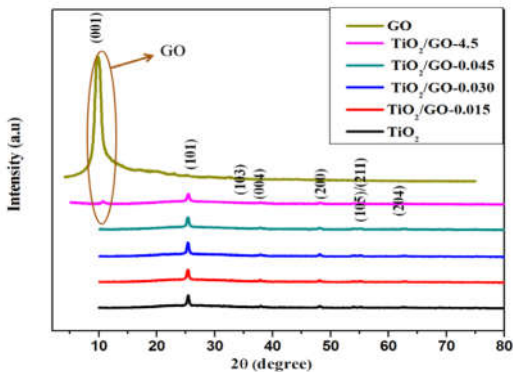


**Fig. 1.** X-ray diffraction patterns of  $\text{TiO}_2$ ,  $\text{TiO}_2/\text{GO}-0.015$ ,  $\text{TiO}_2/\text{GO}-0.030$ ,  $\text{TiO}_2/\text{GO}-0.045$ ,  $\text{TiO}_2/\text{GO}-4.5$  thin films and graphene oxide (GO) nanopowders.

**Table 1:** Structural parameters of  $\text{TiO}_2/\text{GO}$  with different concentration

Samples	$2\theta(^{\circ})$	FWHM	(hkl)	D(nm)
$\text{TiO}_2$	24.68	0.374	(101)	23
$\text{TiO}_2/\text{GO}-0.015$	24.56	0.414	(101)	21
$\text{TiO}_2/\text{GO}-0.030$	24.48	0.426	(101)	20
$\text{TiO}_2/\text{GO}-0.045$	24.36	0.455	(101)	19
$\text{TiO}_2/\text{GO}-4.5$	24.3	0.453	(101)	20

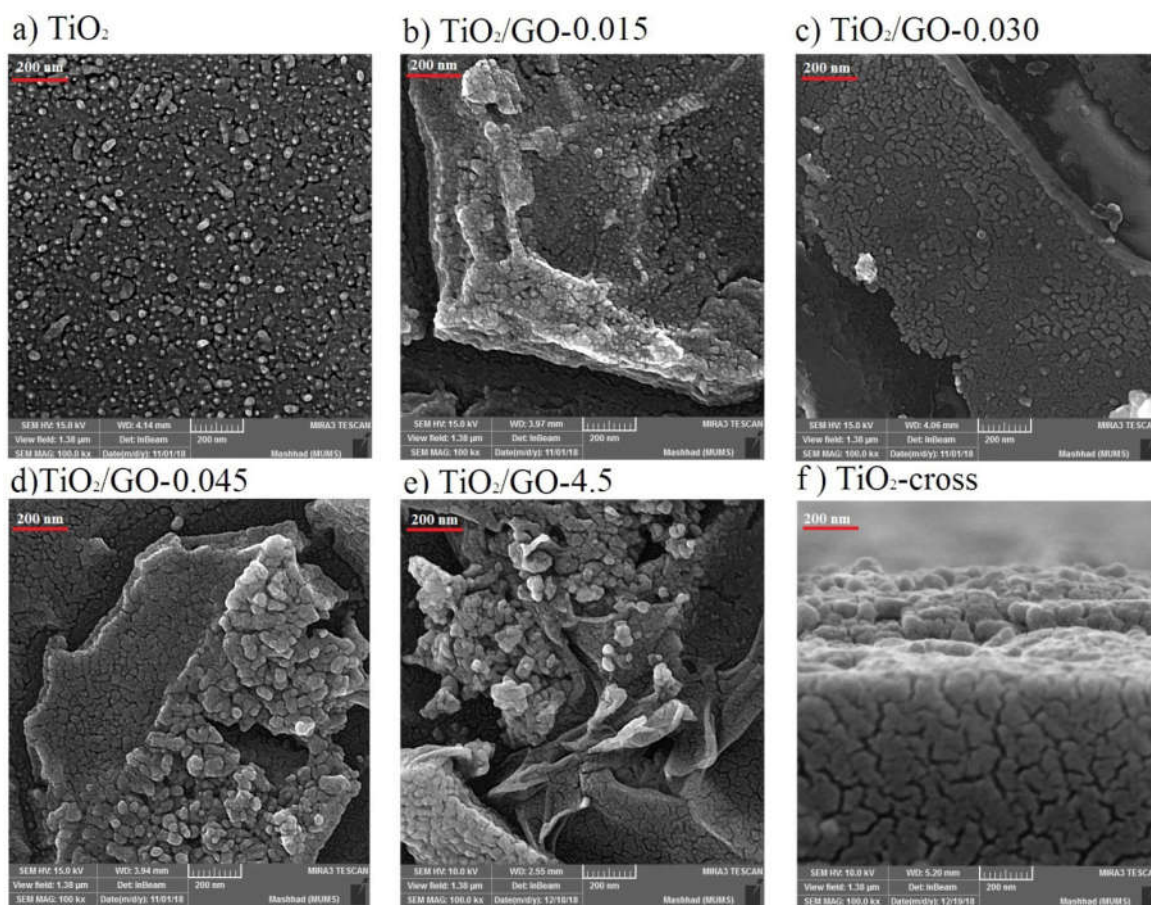


**Fig. 2.** FESEM images of a)  $\text{TiO}_2$ , b)  $\text{TiO}_2/\text{GO}-0.015$ , c)  $\text{TiO}_2/\text{GO}-0.030$ , d)  $\text{TiO}_2/\text{GO}-0.045$ , e)  $\text{TiO}_2/\text{GO}-4.5$  thin films and f) cross-section of  $\text{TiO}_2$  thin film.

In order to identify the chemical elements of thin films, EDS analysis of  $\text{TiO}_2$  and  $\text{TiO}_2/\text{GO}-4.5$  thin films were performed and shown in figure 3. EDX images are used to show the appropriate distribution of particles. Studying the chemical composition of  $\text{TiO}_2/\text{GO}$  thin films was carried out by energy dispersive X-ray (EDX) analysis. As can be seen in the images, the peaks confirm the existence of C, O, and Ti, indicating the formation of a high-purity structure. Peak related to C mainly originates from the GO sheets, while peaks related to Ti belong to  $\text{TiO}_2$  particles. Peak related to O can be formed by  $\text{TiO}_2$  particles and a small number of oxygen groups on RGO sheets. No other peaks were founded in EDX images. Al, Si, and Au are related to the device and materials used for the coating. As it is clear in the FESEM image of  $\text{TiO}_2/\text{GO}-4.5$ , graphene oxide layer almost completely covers  $\text{TiO}_2$  layer; Ti peak intensity in

$\text{TiO}_2/\text{GO}-4.5$  sample decreased and C peak intensity increased, whereas, in pure  $\text{TiO}_2$  sample, the peak intensity increased.

An elevation of the sample surface is recorded by an atomic force microscope (AFM). A 3D image of the desired property is obtained depending on the local interactions. Figure 4 illustrates AFM images of 2D and 3D  $\text{TiO}_2/\text{GO}$  thin films at different concentrations. In  $\text{TiO}_2$  thin layer, the surface of the sample is quite rough due to the grain boundary of  $\text{TiO}_2$  grains (figure 4a). As can be seen,  $\text{TiO}_2$  grains have the same size and morphology. Adding GO layer makes the surface of the samples smoother, and in  $\text{TiO}_2/\text{GO}-4.5$  samples, roughness reached their lowest value (figure 4d). It is evident, that graphene oxide sheets are randomly overlapped. The long wrinkles that also cover the surface of GO-0.045 and GO-4.5 are related to graphene oxide sheets.



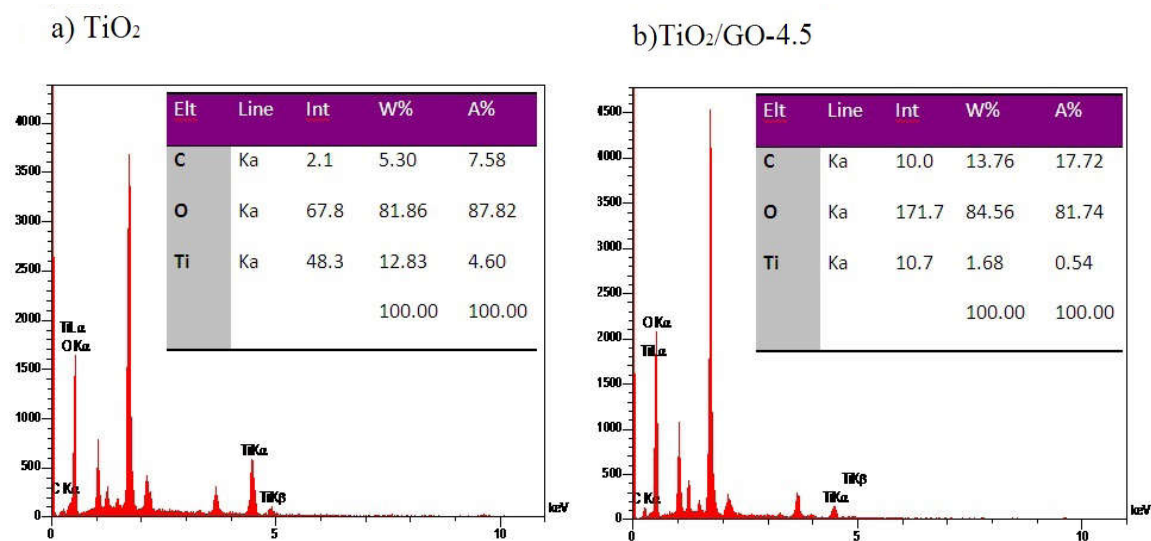
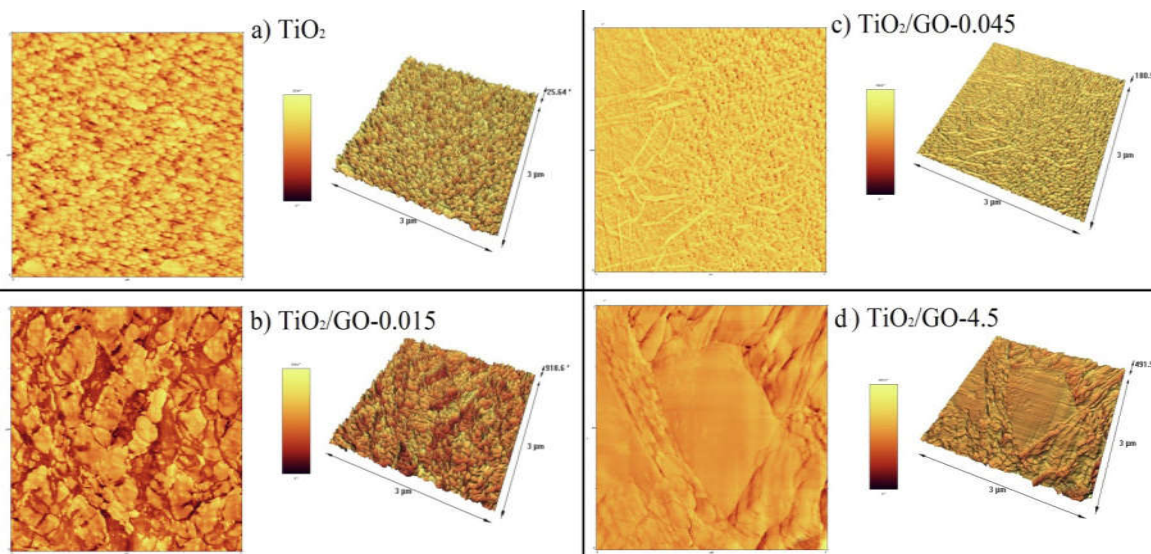
Fig 3. EDS analysis of a) TiO<sub>2</sub> and b) TiO<sub>2</sub>-G4.5 thin films.Fig 4. AFM images of a) TiO<sub>2</sub>, b) TiO<sub>2</sub>/GO-0.015, c) TiO<sub>2</sub>/GO-0.045, d) TiO<sub>2</sub>/GO-4.5 thin films

Fig 5 shows the Raman spectra of TiO<sub>2</sub>/GO-0.015 and TiO<sub>2</sub>/GO-4.5 thin films. Raman peaks at 135 cm<sup>-1</sup>, 392 cm<sup>-1</sup>, 514 cm<sup>-1</sup>, and 634 cm<sup>-1</sup> are referred to E<sub>g</sub>, B<sub>1g</sub>, B<sub>1g</sub>+A<sub>1g</sub>, and E<sub>g</sub> modes, respectively. These peaks are sharp and have good intensity, indicating that TiO<sub>2</sub> microstructure in the deposition process is well crystallized. These peaks have good agreement with the reference values of anatase phase of TiO<sub>2</sub>. The formation of graphene oxide platelets is confirmed by the presence of G and D peaks at 1592 cm<sup>-1</sup> and 1350 cm<sup>-1</sup>, respectively. The G-band is a

characteristic of graphite sheets that confirm the presence of the sp<sup>2</sup> carbon structure. The D-band is related to the existence of defects in the hexagonal structure of graphite. As shown in Figure 5, the intensity of D-band is comparable to the intensity of G-band. Therefore, the graphene oxide layers have significant defects. The disorder degree of carbon structure was specified by calculating the intensity ratio of D/G. As can be seen in AFM and FESEM, in the structure, the ratio of D/G is high, indicating the high degree of irregularity in the structure.



Fig 5. Raman spectra of (a)  $\text{TiO}_2/\text{GO}-0.015$  and (b)  $\text{TiO}_2/\text{GO}-4.5$  thin films.

### 3.2 Photo-Catalyst Properties

The effect of adding the graphene oxide layer on the photocatalytic activity of  $\text{TiO}_2$  has been investigated. The photocatalytic activity of  $\text{TiO}_2/\text{GO}$  at different concentrations was investigated using methyl orange degradation (0.01 mmol/L) in aqueous solution. The films were placed in a methyl orange solution under the stirring and radiation of UV light, which UV light was reflected by two light bulbs with a power of 18 W for 2 hours. The rate of methyl orange degradation was measured using the absorbance spectrum of the solution after 3 hours, which is characterized by UV-Vis spectrometry. The obtained results are shown in figure 6. Adding the graphene oxide layer to the



Fig 6. The UV-Vis spectra of the methyl orange solution in the presence of  $\text{TiO}_2/\text{GO}$  with different concentration of graphene oxide

$\text{TiO}_2$  thin films and increasing its concentration, the amount of light absorption increases in the visible and ultraviolet region. Thus, the amount of methyl orange degradation decreases. As clearly shown in AFM images, by increasing the concentration of graphene oxide, it completely covers  $\text{TiO}_2$  layer, and prevents the penetration of light into  $\text{TiO}_2$  layer and reduces its photocatalytic activity.

### 4.3 Self-Cleaning Effect

The self-cleaning properties of  $\text{TiO}_2$  and  $\text{TiO}_2/\text{GO}$  were investigated and shown in figure 7. Imaging of 10-microliter of water droplet with a magnification of 50 is performed using MZT AM-7013 model of digital camera from Dino-Lite company.

The contact angle of the droplet with the surface in the pure  $\text{TiO}_2$  sample is  $27.24^\circ$ ,  $36.38^\circ$  for left and right angle, respectively, and in  $\text{TiO}_2/\text{GO}-4.5$  sample is equal to  $18.45^\circ$  for left angle and  $19.13^\circ$  for right angle. Researchers have long thought that graphene repels water. However, a new study reported by Belyaeva et al. has revealed that graphene is hydrophilic, not hydrophobic [30]. Accordingly, graphene oxide is hydrophilic; adding graphene oxide layer can reduce the contact angle and increase the hydrophilic properties of the thin film surface. This result is in agreement with the other reports. Safarpour et al. synthesized (rGO)/ $\text{TiO}_2$  nanocomposite thin films to use in nanofiltration by hydrothermal method. Their results show that by increasing the GO weight percentage, the contact angle decreases and their films show the improved hydrophilic properties [31].



Fig 7. The contact angle of the water droplet with a)  $\text{TiO}_2$  and b)  $\text{TiO}_2/\text{GO}-4.5$  surface

### 3.4 Antibacterial Properties

For the antibacterial test, the gram-negative bacteria of the standard *Escherichia coli* (ATCC 25922) (1399 PTCC) was purchased from the Iranian research organization for science and technology. Mueller Hinton broth was prepared from Merck Company.

*Escherichia coli* bacterium was cultured in Muller Hinton broth and incubated at 37 °C for 24 hours. The absorbance\_value of the bacteria cell density was measured at 630 nm in a spectrophotometer. The cell density value was standardized based on the McFarland half (equivalent to  $10^8$  CFU/mL). Antibacterial effect of  $\text{TiO}_2$ ,  $\text{TiO}_2/\text{GO}$ -0.030 and  $\text{TiO}_2/\text{GO}$ -4.5 thin films on the *E. coli* gram-negative bacteria were investigated using microdilution method according to international standard CLSL with three repetitions (figure 8). The absorbance values of the samples at 0, 2, 4, and 20 hr incubation time was measured at 37 °C in the Eliza Reader. The absorption rate of the thin films was compared with positive (bacteria and culture media Mueller Hinton Broth medium) and negative control (Muller Hinton Broth medium). The results indicate that thin films inhibit bacterial growth within 20 hours.  $\text{TiO}_2$  thin film inhibits bacterial growth, but  $\text{TiO}_2/\text{GO}$  thin films show more inhibitory effect. Bacterial growth was inhibited for 2 h incubation at 37 °C.  $\text{TiO}_2/\text{GO}$ -0.030 sample has the highest effect on the inhibition of bacterial growth. By increasing the incubation time, the inhibition of bacterial growth increased simultaneously in comparison with the positive control. Increasing the oxygen pressures for all types of life is harmful and deadly. So,  $\text{TiO}_2/\text{GO}$  thin films, by producing the oxygen free radicals, can create oxidation toxicity for microorganisms using a photo-catalytic material.

Researchers' findings show that graphene materials such as graphene oxide are highly toxic toward bacteria. Graphene oxide has the highest antibacterial activity compared to other graphene structures such as reduced graphene oxide, graphite, and graphite oxide. Antibacterial activity depends on various factors such as time, concentration and size. The

results obtained by Liu et al. show that materials with smaller sizes are more toxic compared to larger materials [32]. For example, the toxicity of graphene oxide is greater than that of graphite oxide. Graphene oxide has a monolayer structure but in graphite oxide the number of layers is very high. Therefore, if the number of layers is lower, it has better antibacterial properties. The examination of the results obtained in this study also confirms these results. The use of graphene oxide increased the antibacterial properties of the layers compared to the titanium dioxide thin film. On the other hand, increasing the concentration of graphene oxide, as seen in the FESEM images, results in a greater number of layers on the surface, thus reducing the antibacterial properties of sample GO-4.5 compared to sample GO-0.03.

Similar results have been reported for other carbon structures. For example, multi-walled carbon nanotubes with a smaller diameter have higher antibacterial activity than larger diameter nanotubes [33-35]. Also, small nC60 aggregates have the greater antibacterial activity than the larger aggregates [36]. Generally, graphene materials that have a higher density of functional groups and are smaller in size have a greater chance of interacting with bacterial cells and thus exhibit better antibacterial activity.

The obtained results are consistent with those of other researchers. Rahimi et al. synthesized  $\text{TiO}_2$ -graphene (TG) nanocomposite with a different percent of graphene using solvothermal method. In the research, photocatalysis activity was studied for disinfection of *E. coli* bacteria. The photo-antibacterial analysis shows that the optical activity is relatively low in this nanocomposite. But, sensitizing the nanocomposite by porphyrin dye material, photo-antibacterial activity increases [37].  $\text{TiO}_2$  nanoparticles and graphene sheets (GSs) composites were also prepared via a direct redox reaction by Cao et al. The obtained results for  $\text{TiO}_2/\text{GSs}$  4.2 wt% show the most photocatalyst antibacterial activity under UV-Visible light radiation. So, it can be used for air and water disinfection [38].

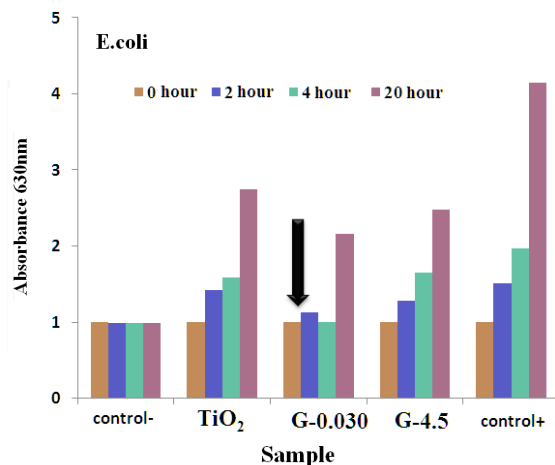


**Fig. 8.** Antibacterial effect of titanium dioxide, TiO<sub>2</sub>/GO-0.030 and TiO<sub>2</sub>/GO-4.5 thin films on the E.Coli gram negative bacteria using microdilution method according to international standard CLSL with three repetitions.

#### 4. CONCLUSION

In the study, the effect of graphene oxide layer addition on TiO<sub>2</sub> thin films has been investigated. TiO<sub>2</sub>/GO thin films at different concentrations are prepared by spin-coating method. The X-ray diffraction pattern shows that titanium oxide with anatase phase is formed. At low concentrations, graphene oxide cannot be seen in the diffraction spectrum, but the graphene oxide peak is shown at 10.5° at 4.5 g/mL concentration. FESEM and AFM images show that by increasing the graphene oxide concentration, it completely covers the titanium oxide layer, so the graphene oxide layer prevents light penetration into the titanium oxide layer, and its photocatalytic activity decreases by adding the graphene oxide. Investigating the contact angle of the layers with water droplets shows that the presence of graphene oxide layer reduces the contact angle and increases the hydrophilic properties of the surface. Studying the effect of adding the graphene oxide on the growth of E.Coli bacteria also shows that the presence of graphene oxide increased the inhibition of bacterial growth.

#### REFERENCES

1. Hashimoto, K., Iril, H. and Fujishima, A., "TiO<sub>2</sub> Photocatalysis: a Historical Overview and Future Prospects", Japanese Journal of Applied Science, 2005, 44, 8269-8285.
2. Guang-lei, T., Hong-Bo, H. and Jian-Da, S., "Effect of microstructure of TiO<sub>2</sub> thin films on optical band gap energy", j chin.phys.lett, 2005, 22, 1787.
3. Malliga, P., Pandiarajan, J., Prithivikumaran, N., and Neyvasagam, K., "Influence of Film Thickness on Structural and Optical Properties of Sol – Gel Spin Coated TiO<sub>2</sub> Thin Film", IOSR Journal of Applied Physics, 2014, 6, 22.
4. López-Heras, I., Madrid, Y. and Cámara, C., "Prospects and difficulties in TiO<sub>2</sub> nanoparticles analysis in cosmetic and food products using a symmetrical flow field-flow fractionation hyphenated to inductively coupled plasma mass spectrometry", j. Talanta, 2014, 124, 71.
5. Saleem, A., Ullah, N., Khursheed, K., Iqbal, T., Shah, S. A., Asjad, M., Sarwar, N., Saleem, M., Arshad, M., "Graphene Oxide–TiO<sub>2</sub> Nanocomposite Films for Electron Transport Applications", Journal of Electronic Materials, 2018, 47, 3749-56
6. Zhu, Y., Shi, J., Zhang, Z., Zhang, C. and Zhang, X., "Development of a Gas Sensor Utilizing Chemiluminescence on Nanosized Titanium Dioxide", j Anal. Chem, 2002, 74, 120.
7. Timoumi, A., Alamri, S. N. and Alamri, H., "The Development of TiO<sub>2</sub>-Graphene oxide Nano composite thin films for solar cells" j. Results in physics, 2018, 3797, 32577.
8. Obeid, B. G., Hameed, A. S., Alaaraji, H. H., "Structural and Optical Properties of TiO<sub>2</sub>:MgO Thin Films Preparing at 373K, Digest Journal of Nanomaterials and Biostructures, 2017, 12, 1239-1246.
9. Shankar, K., Mor, G. K., Prakasam, H. E., Varghese, O. K. and Grimes, C. A., "Self-Assembled Hybrid Polymer-TiO<sub>2</sub> Nanotube Array Heterojunction Solar Cells", Langmuir, 2007, 23, 12445.
10. Zharvan, V., Daniyati, R., Ichzan, N., Yudoyono, and Darminto, S. G., "Study on fabrication of TiO<sub>2</sub> thin films by spin – coating and their optical properties", AIP Conference Proceedings, 2016, 1719, 030018.
11. Démarest, N., Deubel, D., Keromnès, J. C.,



- Vaudry, C., F., Grasset, Lefort, d. R., and Guil-loux-Viryb, M., "Optimization of bandpass optical filters based on  $\text{TiO}_2$  nanolayers", *Optical Engineering*, 2015, 54, 015101.
12. Etefagh, R., Rozati, S. M., Azhir, E., Shahtah-masebi, N., Hosseini, A. S., and Madahi, P., "Synthesis and antimicrobial properties of  $\text{ZnO/PVA}$ ,  $\text{CuO/PVA}$ , and  $\text{TiO}_2/\text{PVA}$  nanocomposites", *Scientia Iranica F.*, 2017, 24, 1717-1723.
13. Kou, Y., Yang, J., Li, B., Fu, S., "Solar photocatalytic activities of porous Nb-doped  $\text{TiO}_2$  microspheres by coupling with tungsten oxide", *Materials Research Bulletin*, 2015, 63, 105-111.
14. Yang, H., Zhang, A. K., Shi, R., Li, X., Dongb, X., Yu, Y., "Sol-gel synthesis of  $\text{TiO}_2$  nanoparticles and photocatalytic degradation of methyl orange in aqueous  $\text{TiO}_2$  suspensions, *Journal of Alloys and Compounds*", 2006, 413, 302-306.
15. Behnajady, M. A. and Eskandarloo, H., "Preparation of  $\text{TiO}_2$  nanoparticles by the sol-gel method under different pH conditions and modeling of photocatalytic activity by artificial neural network. *Research on Chemical Intermediates*", 2015, 41, 2001-17.
16. Fateh, R., Dillert, R. and Bahnemann, D., "Self-cleaning properties, mechanical stability, and adhesion strength of transparent photocatalytic  $\text{TiO}_2\text{-ZnO}$  coatings on polycarbonate". *ACS applied materials & interfaces*, 2014, 6, 2270-8.
17. Jozee, M. Saadat Mahmoudi, Sanjabi, S. and Mirzaee, O., "Electrophoretic Deposition of  $\text{TiO}_2$ -Multi-Walled Carbon Nanotube Composite Coatings: Morphological Study". *Iranian Journal of Materials Science & Engineering*, 2016, 13, 39-44.
18. Jumeri, F. A., Lima, H. N., Zainal, Z., Huang, N. and Pandikumar, M., A., "Titanium dioxide-reduced graphene oxide thin film for photo-electrochemical water splitting", *Ceramics International*, 2014, 40, 15159-15165.
19. Sahnesarayi, M., Karimi, Sarpoolaky, H. and Rastegari, S., "Influence of Multiple Coating and Heat Treatment Cycles on the Performance of a Nano- $\text{TiO}_2$  Coating in the Protection of 316L Stainless Steel Against Corrosion under UV Illumination and Dark Conditions". *Iranian Journal of Materials Science & Engineering*, 2019, 16, 33-42.
20. Wang, Z., Helmersson Kall, U., "Optical properties of anatase  $\text{TiO}_2$  thin films prepared by aqueous sol-gel process at low temperature", *Thin Solid Films*, 2002, 405, 50-54.
21. Sharma, A., Karn, R. K., Pandiyan, S. K., "Synthesis of  $\text{TiO}_2$  Nanoparticles by Sol-gel Method and Their Characterization", *Journal of Basic and Applied Engineering Research*, 2014, 1, 1-5.
22. Woan, K., Pyrgiotakis, G., Sigmund, W., "Photocatalytic Carbon-Nanotube- $\text{TiO}_2$  Composites", *Advanced Materials*, 2009, 21, 2233.
23. Safarpour, M., Vatanpour, V., Khataee, A. and Esmaeili, M., "Development of a novel high flux and fouling-resistant thin film composite nanofiltration membrane by embedding reduced graphene oxide/ $\text{TiO}_2$ ". *Separation and Purification Technology*, 2015, 154, 96-107.
24. Mahmood, H., Habib, A., Mujahid, M., Tanveer, M. and AsifJamil, S., "Materials Sciencein Semiconductor Processing", 2014, 24, 193-199.
25. Shahriary, L. and Athawale, A., "Graphene Oxide Synthesized by using Modified Hummers Approach", *International Journal of Renewable Energy and Environmental Engineering*, 2014, 2, 32.
26. Baig, M. I., Ingole, P. G., Jeon, J., Hong, S. U., W. K. and Lee, H. K., "Water vapor transport properties of interfacially polymerized thin film nanocomposite membranes modified with graphene oxide and GO- $\text{TiO}_2$  nanofillers", *Chemical Engineering Journal*, 2019, 373, 1190-1202.
27. Becerril, H., Mao, J., Liu, Z., Stoltenberg, R. M., Bao, Z. and Chen, Y., "Evaluation of Solution-Processed Reduced Graphene Oxide Films as Transparent Conductors", *American Chemical Society*, 2008, 2, 463.
28. Hosseini, S. M., Ghanbari Shohany, B., Azad, N., and Kompany, A., "Electrical properties comparison of NTC thermistors prepared from nanopowders and in mixed oxide process", *Materials Science-Poland*, 2011, 29, 253.
29. Belyaeva, L. A., Van Deursen, P. M. G., Barbet-sea, K. I. and Schneider, G. F., "Hydrophilicity of Graphene in Water through Transparency to Polar and Dispersive Interactions", *Adv. Mater*, 2018, 30, 1703274.
30. Rahimi, R., Zargari, S., Yousefi, A., Berijani, M. Y., Ghaffarinejad, A. and Morsali, A., "Visible light photocatalytic disinfection of E. coli with  $\text{TiO}_2$ -graphene nanocomposite sensitized with tetrakis (4-carboxyphenyl) porphyrin", *Applied Surface Science*, 2015, 355, 1098-106.

31. Liu, S., Zeng, T. H., Hofmann, Burcombe, M., Wei, E., Jiang, J., Kong, R. and Chen, J. Y., "Antibacterial Activity of Graphite, Graphite Oxide, Graphene Oxide, and Reduced Graphene Oxide: Membrane and Oxidative Stress", *ACS nano*, 2011, 5, 6971–6980.
32. Kang, S., Herzberg, M., Rodrigues, D. F. and Elimelech, M., "Antibacterial Effects of Carbon Nanotubes: Size Does Matter", *Langmuir*, 2008, 24, 6409–6413.
33. Kang, S., Mauter, M. S. and Elimelech, M., "Physicochemical, Determinants of Multiwalled Carbon Nanotube Bacterial Cytotoxicity", *Environ. Sci. Technol*, 2008, 42, 7528–7534.
34. Liu, S. B., Wei, L., Hao, L., Fang, N., Chang, M. W., Xu, R., Yang, Y. H. and Chen, Y. "Sharper and Faster Nano Darts Kill More Bacteria: A Study of Antibacterial Activity of Individually Dispersed Pristine Single-Walled Carbon Nanotube", *ACS Nano*, 2009, 3, 3891–3902.
35. Lyon, D. Y., Adams, L. K., Falkner, J. C. and Alvarez, P. J. J., "Antibacterial Activity of Fullerene Water Suspensions: Effects of Preparation Method and Particle Size", *Environ. Sci. Technol*, 2006, 40, 4360–4366.
36. Cao, B., Cao, S., Dong, P., Ga, J. and Wang, J., "High antibacterial activity of ultrafine TiO<sub>2</sub>/graphene sheets nanocomposites under visible light irradiation", *J Materials Letters* 2013, 93, 349–352.
37. Shahriary, L. and Athawale, A. A., "Graphene Oxide Synthesized by Using Modified Hummers Approach", *International Journal of Renewable Energy and Environmental Engineering*, 2014, 2, 58-63.